J. Int. Environmental Application & Science, Vol. 16(1): 1-11 (2021)
Research Paper

Investigation on Adsorption Properties of Egg White Protein Polymers Using a Model Azo Dye Amaranth

Ayşe Dinçer[1*], Pelin Bedriye Karanfil[1], Esra Menfaatli[2], Figen Zihnioğlu[2]

[1]*Manisa Celal Bayar University, Faculty of Science and Arts, Chemistry Department, Yunusemre Manisa Turkey;* [2]*Ege University, Faculty of Science, Biochemistry Department, Bornova, İzmir, Turkey.*

Received September 09, 2019;Received January 05, 2020; Accepted February 04, 2021

Abstract: Eco-friendly egg white protein polymers (EWPP) were used as an adsorbent for removal amaranth dye efficiently. Dye binding conditions (pH, initial dye concentration temperature and contact time) were optimized, and it was seen that the pH had a pronounced effect on the adsorption of amaranth on EWPP. The experimental amaranth binding capacity of EWPP was increased from 38 mg/g to 65.56 mg/g as the contact time increased from 10 min to 50 min. The experimental study correlated with the Freundlich isotherm and well defined by the pseudo-second-order kinetics. ΔG^o, ΔH^o, and ΔS^o values were calculated as -2.19 kJ/mol, -23.24 kJ/mol, and -69.3 kJ/K.mol at 25 °C, respectively. The adsorption of amaranth dye on egg white-based polymer was demonstrated to be exothermic. The characterization of EWPP was done by using a scanning electron microscope (SEM) analysis.

Keywords: *Amaranth, dye adsorption, egg white protein polymer, isotherms, kinetics,*

Introduction

One of the major problems of the modern world is water pollution. Wastewaters from agricultural, urban and, industrial activities causes significant pollution of streams and rivers (Long, 2020). There are many pollutant sources like surfactants (Siyal *et al*., 2020), dyes (Sohni *et al*., 2019), and heavy metal ions (Soliman & Moustafa, 2020). Dyes in wastewaters are one of the important pollution problems for the environment. They have long been used in many industries like food industries, leather, dyeing paper and pulp, plastics, textiles, and cosmetics (Chiou & Li, 2002; Zhou *et al*., 2014). Decolorizing hazardous dyes is difficult due to their complex structure. Dyes are resistant to natural degradation by light and microorganisms. Penetration of sunlight into the water is prevented, and they inhibit the photosynthetic activity of aquatic plants (Wong et al. 2018). Many of them have aromatic and azo groups, and they have negative effects on health (Mittal *et al*., 2010; Ge *et al*., 2012). Scientists focus on finding a solution for the removal of pollutants effectively. There are many dye removal techniques such as electrochemical methods, filtration, biodegradation, coagulation, and adsorption (Wang *et al*., 2020). Adsorption technique has applications for environmental pollution control because it is economic, efficient, and faster than other techniques (Long *et al*., 2021).

Dyes can be classified as acidic and basic dyes according to their functional groups. Amaranth is a water-soluble acidic mono azo dye, and it has a dark red color ($C_{20}H_{11}N_2Na_3O_{10}S_3$). It is used as a colorant in the food industry and cosmetics. Although it is non-mutagenic at low concentrations (Liu et al. 2020b), it may cause some problems on health such as birth defects, respiratory problems, allergy, and tumors in humans when used at high concentrations and prolong time (Abdellaoui et al. 2017; Lin and Wu 2017; Ndifor-Angwafor et al. 2017; Liao and Wang 2018). Its solubility and stability in water are very high, and the removal of amaranth dye from wastewaters is difficult by common methods. The removal of amaranth is important for protecting the health of living organisms. There are some papers about the adsorption of amaranth such as using layered double hydroxides (Abdellaoui *et al*., 2017), tamarind pod shells (Ahalya et al. 2014), water hyacinth (Guerrero-Coronilla *et al*., 2014), nanoparticles composed Cu_2O microspheres (Liao & Wang 2018), poly(NIPAm/LMSH) nanocomposite hydrogels (Bai *et al*., 2016), and Fe_3O_4/MgO nanoparticles (Salem et al. 2016), functionalized graphene oxide aerogels (Xu *et al*., 2020) and 3D hierarchical layered double hydroxide/carbon spheres (Lyu *et al*., 2020). Egg white protein has a nutritional value and has an expanded application area in food industries. Also, it can be used for different uses such as enzyme immobilization support (Wahba 2020), preparation

*Corresponding: E-Mail: ayse.dincer@cbu.edu.tr; Tel: +90 236 2013173; Fax: +90 236 2013040

of the flame retardant cellulosic fabrics (Liu et al. 2020a), and preparation of composite films (Huang *et al*., 2020).

In this study, efficient removal of amaranth was done using EWPP as an adsorbent. The preparation of the adsorbent is easy and economic. The influences of pH, initial amaranth concentration, temperature, and contact time on dye binding were investigated. The thermodynamics, isotherm, and kinetics studies were studied to understand amaranth binding on EWPP. SEM analysis was performed for morphologic characterization.

Materials and Methods

Amaranth (KRK Gıda, Istanbul, Turkey (Figure 1)). Chicken eggs were purchased from a local market. Glycine, glutaraldehyde, ether, acetic acid, acetone, sodium hydroxide, methanol, and hydrochloric acid (Sigma Aldrich (USA)).

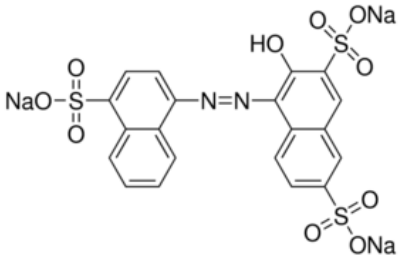

Figure 1. Molecular structure of amaranth dye.

Spectrophotometric analysis

Aqueous standard solutions of amaranth dye were prepared in the 5-15 mg/L concentration range. Dye removal studies were monitored spectrophotometrically at 520 nm.

Preparation of EWPP

EWPP was prepared by slowly adding ice-cold acetone to egg white (80 mg/mL protein) with a ratio of 1:1 under stirring conditions. The resulting protein-acetone suspension was kept at -20 ℃ for 30 minutes for complete precipitation and then aggregates were cross-linked using 200 mM glutaraldehyde for 30 minutes. Free aldehyde groups on the polymer blocked with 0.5 M glycine. Finally, EWPP was washed with distilled water, ether, methanol, and acetone respectively, and dried at room temperature before use.

Characterization of EWPP

Morphology characterization of EWPP was done using SEM (Quanta 250 FEG/FEI). Before taking measurements, EWPP was vacuum dried and coated with a gold thin film.

Adsorption studies

To determine the maximum amaranth dye binding capacity of EWPP, batch adsorption experiments were performed at different pH, contact time, temperature, and initial dye concentrations values. The pH of the adsorption medium was set to pH 1.0 to 4.0. The effect of initial dye concentration was examined in 40-500 mg/L. Temperature effect was studied at various temperature values (25-50°C) accompanied by mild shaking. The effect of contact time was determined at different dye concentrations (40-300 mg/L) by changing the time of contact from 1 to 50 min. EWPP-dye solution suspension was centrifugated at 10000 rpm then the absorbance of unbound dye in the supernatant was determined spectrophotometrically.

Eq 1 was used to find the amount of dye bound on EWPP:

$$qe = \frac{(Co - Ce)\, x\, V}{m} \quad (1)$$

qe: The amount of amaranth adsorbed (mg/g),

C_o : The initial amaranth concentration (mg/L)

Ce : The equilibrium amaranth concentration (mg/L)

V : The volume of solution (L)

m: The amount of EWPP (g)

Desorption of the EWPP

The regeneration and reuse of an adsorbent are critic parameters for economic feasibility. Desorption studies of the dye adsorbed EWPP was performed by 0.1 M NaOH: MeOH (1:1 v/v).

Results and Discussion

Morphologic Analysis of EWPP

The preparation steps of the EWPP and the appearance of the medium contains dye before and after adsorption is displayed in Fig. 2. SEM is used to characterize the surface morphology and physical properties (Hussien et al. 2016). EWPP has a rough and porous character providing an increased surface area. Dye binding capacity of EWPP was highly affected by the polymer's surface structure and it exhibited higher adsorption capacity (Fig. 2).

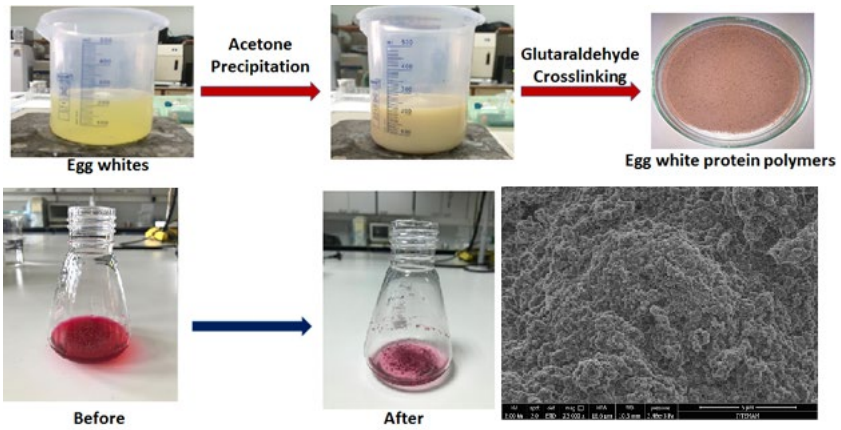

Figure 2. Preparation steps and SEM micrograph of EWPP

Adsorption Studies

The pH of the dye solution has a critical role on binding. To investigate the effect of pH, the pH of the solution set to pH 1.0-4.0 by 0.1 M HCl. Dye adsorption on EWPP highly dependend on the pH of the medium. The highest dye uptake occurred at pH 2.0. As pH increased from 1.0 to 4.0, dye binding capacity of EWPP was decreased sharply (Figure 3A). Amaranth is a mono azo dye and has three sulfonic acid groups. These groups are negatively charged at pH 2.0 and could be interacted with the positive charges of EWPP. Below pH 4.0, the adsorption of amaranth on EWPP could be favorable because of significantly high electrostatic forces. The charge of the EWPP had changed when pH was increased. The electrostatic repulsion occurred at high pH values so the adsorption rate of the dye decreased. The adsorption capacity was calculated as 8.94 mg/g when 20 mg EWPP was treated with 40 mg/L amaranth dye solution at pH 2.0. Angwafor et al reported that the maximum amaranth dye binding on lignocellulosic materials had occurred at pH 2.0 (Ndifor-Angwafor et al. 2017). Ahalya et al. (Ahalya et al. 2014), Ahmad and Kumar (Ahmad and Kumar 2011) also found pH 2.0 for the maximum adsorption of amaranth dye on tamarind pod shells and alumina reinforced polystyrene, respectively. Bai et al. reported that amaranth binding on NPX nanocomposite hydrogel was more effective in pH 2.0 (Bai et al. 2016).

The experimental dye capacity of EWPP was determined by taking measurements at different concentrations of amaranth dye solution (40-500 mg/L, pH 2.0). The amount of dye bonded was low below 40 mg/L and as the initial dye concentration was increased the amount of the dye bound was increased. Equilibrium was reached when amaranth concentration increased to 250 mg/L and subsequently remained unchanged (Figure 3B). This may be because of a driving force of the concentration gradient (Chiou and Li 2002; Sun et al. 2010). The experimental amaranth dye binding capacity was calculated as 38 mg/g when the contact time was 10 min.

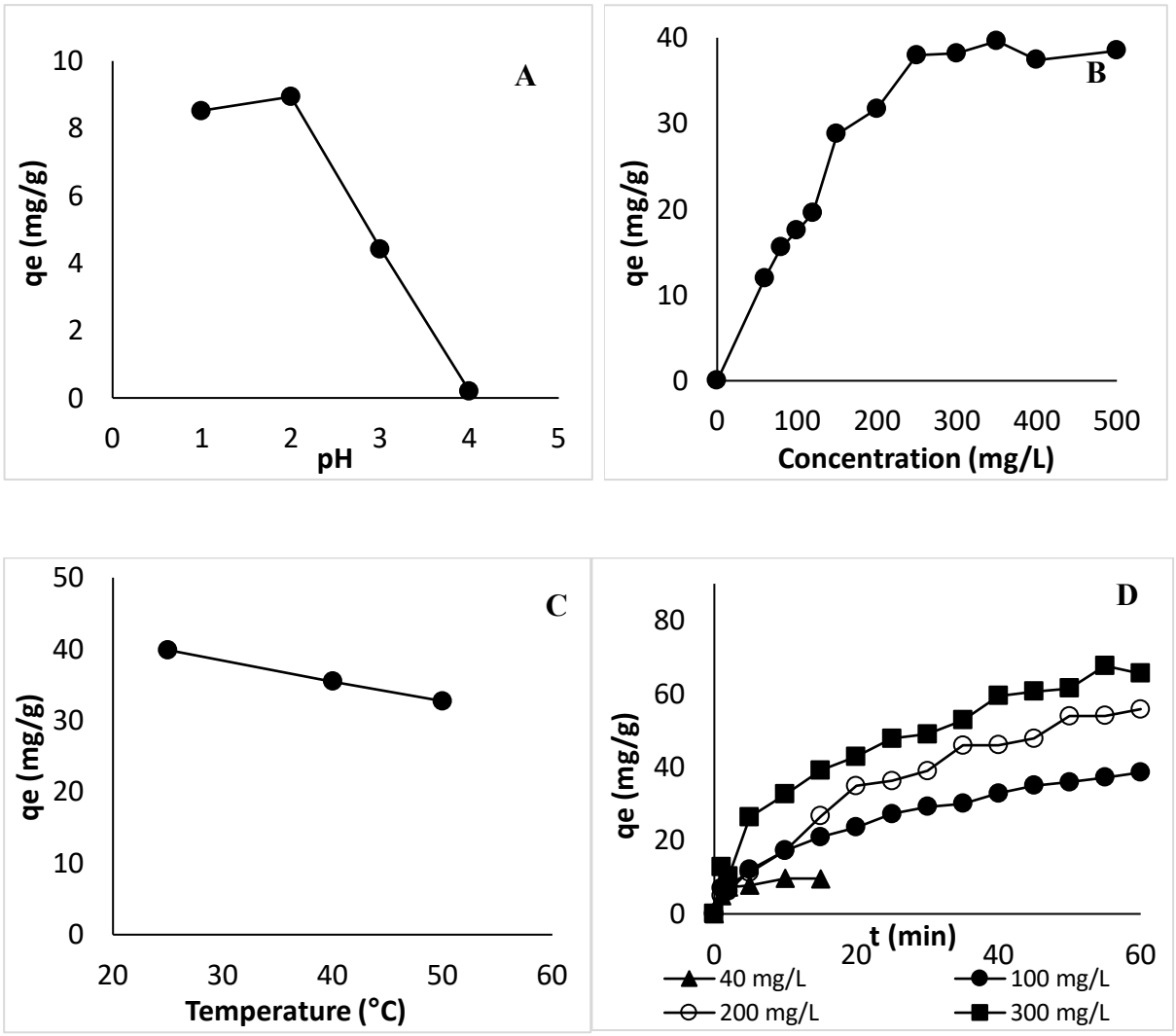

Figure 3. (A) Effect of pH *(Conditions: 20 mg EWPP, 40 mg/L amaranth dye, V: 4 mL, adsorption time: 30 min, temperature: 25 °C).* ***(B)*** *Effect of initial amaranth dye concentration (Conditions: 20 mg EWPP, V: 4 mL, pH 2.0, temperature:25 °C, adsorption time: 10 min).* ***(C)*** *Effect of temperature (Conditions: 20 mg EWPP, 250 mg/L amaranth dye, V: 4 mL, pH 2.0, adsorption time: 10 min)* ***(D)*** *Effect of contact time (Conditions: 20 mg, EWPP, 40 mg/L-300 mg/L amaranth dye, V: 4 mL, pH 2.0; temperature: 25 °C).*

To examine the temperature effect of, 250 mg/L amaranth dye solution (pH 2.0) was added to EWPP and shaken gently at various temperature values (25-50 °C) for 10 min. The adsorption amount of amaranth dye was slightly decreased when the temperature changed from 25 to 50 °C (Figure 3C). Maximum amaranth adsorption occurred at 25 °C. At high temperatures, the solubility of the amaranth dye was affected and stronger interactions occurred between dye and water than EWPP. Brownian movement of amaranth dye in water was increased as the temperature was increased and so the adsorption amount of amaranth dye was decreased (Aljeboree *et al*., 2017). The adsorption of amaranth is controlled by an exothermic reaction.

Determination of optimum contact time is important step in optimizing the dye binding conditions. For this purpose, 20 mg of EWPP was added to 40-100-200-300 mg/L amaranth dye solution (pH 2.0) and measurements were taken between 1-50 min. As seen from Figure 3D, the adsorption kinetics of amaranth dye was very fast when 40 mg/L amaranth dye was used and reached the equilibrium in 10 min. As the concentration of amaranth was changed from 40 to 300 mg/L, the dye binding capacity of EWPP was also changed from 38 mg/g to 65.56 mg/g. The time required for the adsorption to come to equilibrium changed from 10 min to 50 min. Bai et al. also observed similar results for adsorption amaranth on NPX nanocomposite hydrogels (Bai *et al*., 2016).

Thermodynamic parameters

The thermodynamic parameters were determined using Eq. 3 and 4:

$$\ln Kc = \frac{\Delta S^{\circ}}{R} - \frac{\Delta H}{RT} \quad (3)$$

$$\Delta G = -RT ln\, Kc \quad (4)$$

where Kc= (C_A/Ce) is the adsorption equilibrium constant, C_A is the amount of amaranth bound on EWPP at equilibrium (mg/L); Ce is the equilibrium concentration of the amaranth in the solution (mg/L). T (K) is the absolute temperature, R is the gas constant. ΔH^0 and ΔS^0 values were found from the slope and intercept of the graphic of ln Kc versus 1/T. The related parameters were calculated and given in Table 1. The negative ΔG^0 values indicated the adsorption is thermodynamically feasible and spontaneous in the studied temperature values. The negative ΔH^0 shows the adsorption of the dye is exothermic. A negative ΔS^0 value shows the decrease in randomness on the adsorption.

Table 1. Thermodynamic parameters of amaranth dye adsorbed on EWPP

T (K)	ΔG (kj/mol)	ΔS (kj/mol.K)	ΔH (kj/mol)
298K	-2.19	-69.3	-23.24
313K	-1.63		
323K	-0.87		

Adsorption isotherms

In many papers, the experimental data was evaluated by adsorption isotherms such as Langmuir, Freundlich, and Temkin models (Annadurai et al. 2002; Ghaedi et al. 2012; Chen et al. 2019; Godiya et al. 2019; Shi et al. 2020; Mishra et al. 2021). Eq. 6 is used to define Freundlich model:

$$\log qe = \log K_F + 1/n \log Ce \quad (6)$$

where qe is the amount of the dye bonded, K_F and n are defined as the adsorption capacity and the adsorption intensity respectively. 1/n and K_F values were found from the slope and intercept of the graphic drawn between log qe and log Ce.

Langmuir equation is defined as (Equation 7):

$$\frac{Ce}{qe} = \frac{1}{Q_{max}.b} + \frac{Ce}{Q_{max}} \quad (7)$$

where Q_{max} is the maximum amaranth binding capacity of EWPP (mg/g), and Langmuir isotherm constant, b (L/mg) relates to adsorption energy.

Dimensionless R_L (separation factor) is used to analyze the adsorption process. R_L can be expressed as:

$$R_L = 1/(1+bC_0) \quad (8)$$

Where b is the Langmuir constant and C_0 is the initial dye concentration (mg/L)

If the R_L value is between 0 and 1, this means the adsorption process is favorable, if R_L>1, it shows unfavorable adsorption. If R_L=1 or R_L=0, it shows the adsorption process linear or irreversible respectively (El-Naggar et al. 2018). R_L value for the adsorption of amaranth onto EWPP was calculated as 0.0039, showing that the dye binding process was favorable.

Temkin isotherm considers the adsorbent and the adsorbate molecules indirectly interact on adsorption isotherms (Shi et al. 2020). Eq. (9) is used to define Temkin isotherm:

$$qe = \frac{RT}{b} \ln A_T + \left(\frac{RT}{b_T}\right) lnC_e \quad (9)$$

B=RT/b and corresponded to adsorption enthalpy, R is the gas constant (8.314×10^{-3} kJ/mol.K), b is the Temkin constant related to the adsorption heat (kJ/mol), and A_T is the maximum binding energy at equilibrium (L/g).

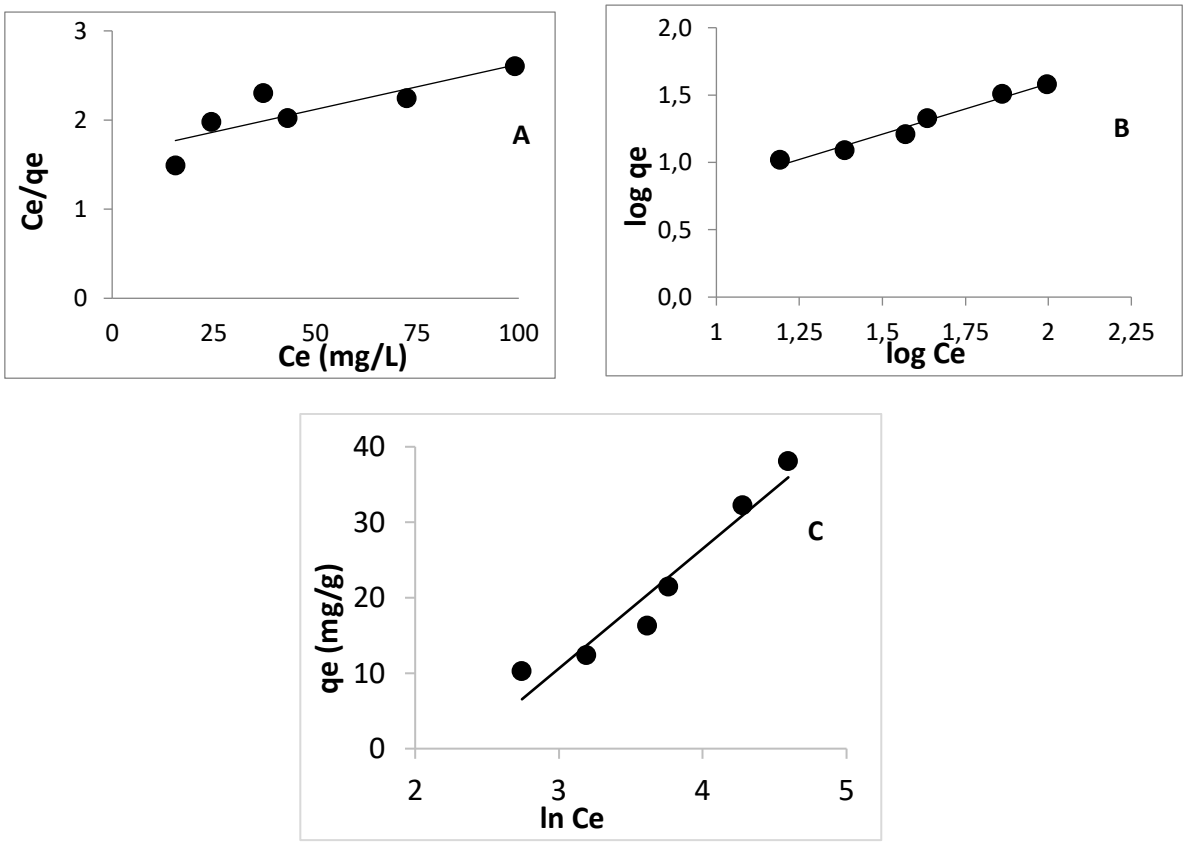

Figure 4: Langmuir (A), Freundlich (B), and Temkin (C) isotherm graphs of amaranth adsorption

Table 2. Adsorption isotherm parameters of amaranth dye adsorbed on EWPP

Isotherm Models		
Langmuir	**Freundlich**	**Temkin**
R^2=0.7208	R^2=0.9734	R^2=0.9352
qmax=98.04 mg/g	K_F=1.21 ((mg/g)(L/mg)$^{1/n}$)	A=0.0973 L/g
b=0.0063 L/mg	n=1.33	b=0.156 kj/mol
R_L=0.0039		B=15.872

Adsorption profiles of three adsorption isotherms and related parameters are displayed in Figure 4 and Table 2. When the R^2 values were compared, the adsorption behavior amaranth on EWPP is well described by Freundlich isotherm. The obtained results show that EWPP has a heterogeneous surface for the binding of amaranth. The exponent 1/n value is the indicator of the adsorption process. If the n value is higher than 1, it shows the adsorption process is favorable. In this work, the n value was calculated as 1.33, which means that the adsorption of amaranth on EWPP is favorable. EWPP has higher amaranth binding capacity than some stated adsorbents (Table 3).

Table 3: The amaranth binding capacities of some adsorbents.

Adsorbents	**Q (mg/g)**	**References**
EWPP	98.04	This study
Fe_3O_4@mZrO_2/rGO	76.9	(Jiang *et al*. 2014)
Fe_3O_4/MgO nanoparticles	38.1	(Salem *et al*. 2016)
Tamarind pod shells	65.04	(Ahalya *et al*. 2014)
Untreated pineapple peeling	31.25	(Ndifor-Angwafor *et al*. 2017)
MgO microcubes	43.74	(Li *et al*. 2019)
Sulfobetaine-modified magnetic nanoparticles	57.01	(Qiao *et al*. 2019)
Spherical ZnO nanoparticles	74.02	(Zafar *et al*. 2019)

Kinetics analysis

The adsorption kinetics parameters of EWPP is calculated for 100 mg/L, 200 mg/L and 300 mg/L amaranth concentrations. Sorbent material's performance is determined by the pseudo-first-order and pseudo-second-order kinetics (Equation 9 and 10) (Ho and McKay 1998).

$$\log(qe - qt) = \log qe - \frac{k_1}{2.303} t \quad (9)$$

$$\frac{t}{qt} = \frac{1}{k_2\, qe^2} + \frac{t}{qe} \quad (10)$$

where qt (mg/g) is the dye binding capacity on EWPP at any given time t (min). k_1 (min^{-1}) is the pseudo-first-order rate constant, and k_2 (g mg^{-1} min^{-1}) is the pseudo-second-order model rate constant.

The graphics and calculated kinetic parameters of amaranth adsorption on EWPP are shown in Figure 5 and Table 4 respectively. The experimental adsorption capacities were found as 38.56, 55.8, and 65.56 mg/g for 100 mg/L, 200 mg/L, and 300 mg/L dye concentrations after 50 min incubation, respectively. The calculated equilibrium binding capacities (qe) for the pseudo-first-order kinetic model are 37.14 mg/g, 58.45 mg/g, and 59.25 mg/g for three dye concentrations, respectively. It was significantly lower than calculated qe values of the pseudo-second-order kinetics. When the R^2 values are compared for three concentrations of amaranth dye, the adsorption is correlated with the pseudo-second-order kinetics.

Weber's intra-particle diffusion model used for determining the rate-limiting step (Weber and Chakravorti 1974)

$$qt = K_{id} t^{1/2} + C$$

where K_{id} (mg g^{-1} min$^{-1/2}$) is the rate constant of intraparticle diffusion, and C is the intercept which describes the boundary layer thickness (mg/g). When the plots were drawn according to the intra-particle diffusion model, the straight lines were obtained but none of them passed through the origin (Fig.5). This means that other processes affect the adsorption besides intraparticle diffusion (Ghaedi et al. 2012; Pandian et al. 2013). Intraparticle rate constant (K_{id}) values were increased from 4.95 mg/g.min$^{1/2}$ to 8.26 mg/g.min$^{1/2}$, as the initial dye concentration was changed from 100 to 300 mg/L.

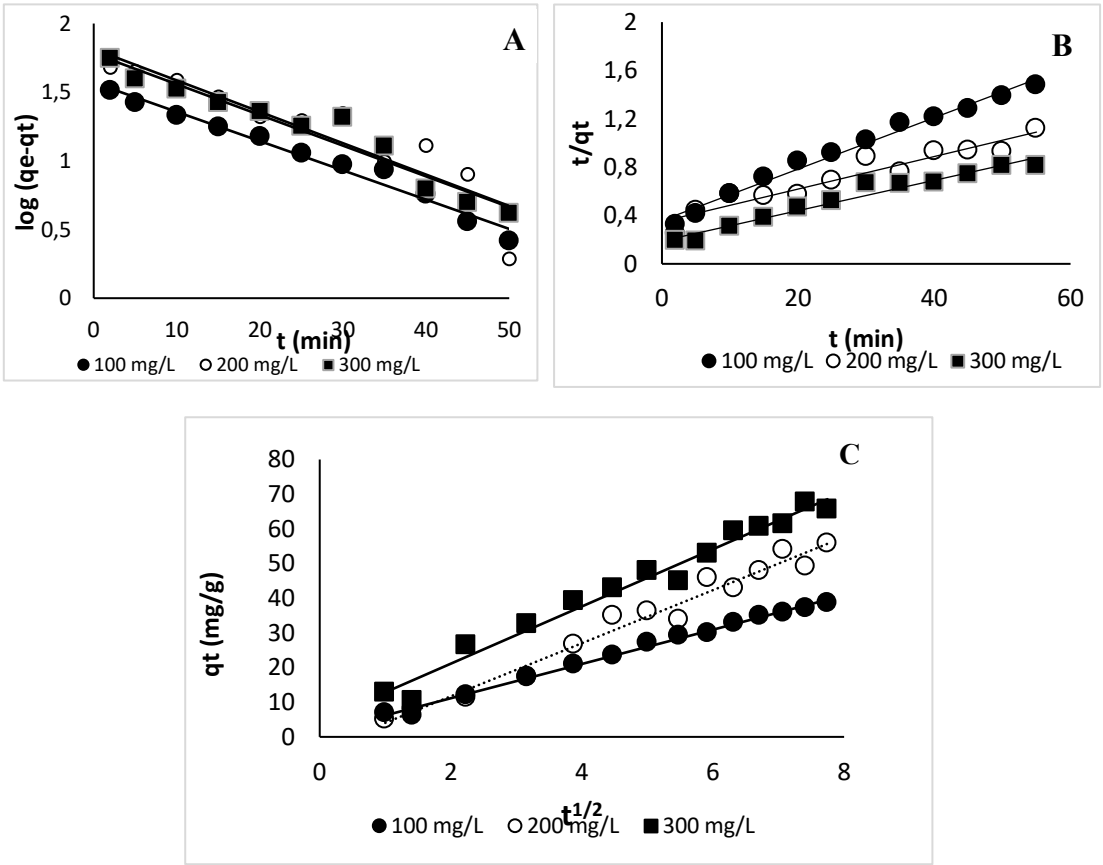

Figure 5. Pseudo-first-order (A), pseudo-second-order (B) kinetics, and intraparticle effect (C) of amaranth adsorption on EWPP.

Table 4. Kinetic parameters of amaranth dye adsorbed on EWPP

Dye Concentration	100 mg/L	200 mg/L	300 mg/L
Pseudo first -order kinetics	R^2=0.9761 qe=37.14 mg/g k_1=0.049 min^{-1}	R^2=0.8378 qe=58.45 mg/g k_1=0.047 min^{-1}	R^2=0.943 qe=59.25 mg/g k_1=0.051 min^{-1}
Pseudo second-order kinetics	R^2=0.9849 qe=45.87 mg/g k_2=1.32.10^{-3} g/mg.min	R^2=0.912 qe=74.07 mg/g k_2=5.21.10^{-4} g/mg.min	R^2=0.9614 qe=80 mg/g k_2=8.24.10^{-4} g/mg.min
Intraparticle diffusion effect	R^2=0.9937 K_{id}=4.95 mg/g.$min^{1/2}$ C=1.25	R^2=0.9724 K_{id}=7.66 mg/g.$min^{1/2}$ C=-3.6	R^2=0.9759 K_{id}=8.26 mg/g.$min^{1/2}$ C=4.6

Reusability of EWPP

The changes in the binding capacity of the EWPP for the amaranth dye after five adsorption-desorption cycles were seen in Figure 6. In the first adsorption step, the calculated dye binding capacity was 38 mg/g. Using 0.1 M NaOH: MeOH (1:1), desorption of the dye was done. This solution causes deprotonation of the positively charged amino groups of EWPP and weakens the electrostatic interaction between amaranth and EWPP. After five cycles, the dye binding capacity of EWPP was decreased by about 67%.

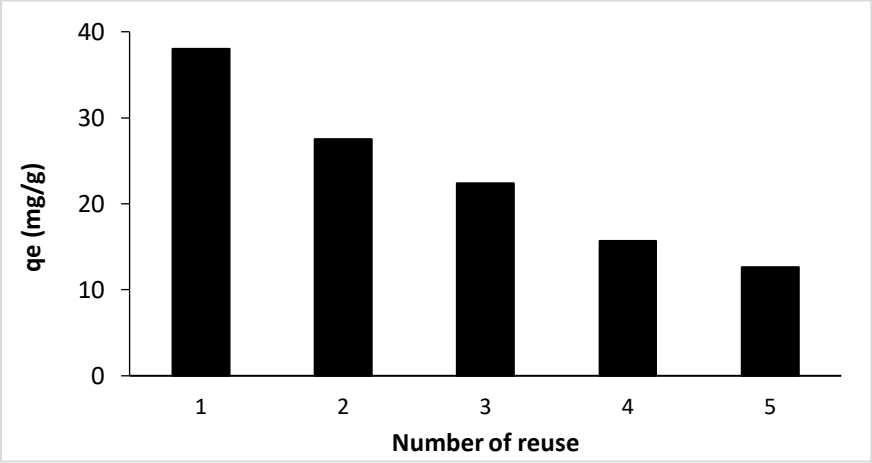

Figure 6. Changes in the adsorption capacity of EWPP after five adsorption cycles

Conclusion

Water is a very important component of living organisms and pollution of water resources puts their health at risk. There are many resources of pollution and dyes are one of them. Dyes are used in many areas of industry and their removal from water is difficult. The adsorption technique is one of the most applied techniques for removing pollutants and finds an application area for dye removal. It is cheap, economic and also various kinds of adsorbents can be used. In this work, EWPP as an adsorbent successfully removed the amaranth dye from an aqueous solution. This adsorbent was easily prepared by precipitating the egg white protein in the presence of cold acetone and then crosslinked with glutaraldehyde. EWPP is an eco-friendly adsorbent and has many functional groups that may interact with dye molecules. It can be used for dye removal from wastewaters. Adsorption experiments showed that pH highly affected the binding of amaranth on EWPP because of the high electrostatic interactions. An increase in the temperature negatively affected the sorption of the amaranth, and for this reason, 25 °C was chosen as an optimum adsorption temperature. Thermodynamic parameters were calculated, ΔG and ΔH values were negative therefore the dye binding process was spontaneous and exothermic. Adsorption process was suited Freundlich isotherm, and the adsorption kinetics was fitted to the pseudo-second-order.

References

Abdellaoui K, Pavlovic I, Bouhent M, Benhamou A, Barriga C,, (2017) A comparative study of the amaranth azo dye adsorption/desorption from aqueous solutions by layered double hydroxides. *Appl. Clay. Sci.* **143**, 142–150. https://doi.org/10.1016/j.clay.2017.03.019

Ahalya N, Chandraprabha MN, Kanamadi RD, Ramachandra TV, (2012) Adsorption of Methylene Blue and Amaranth on to tamarind pod shells. *J. Biochem. Technol.* **3(5)**, S189–S192.

Ahmad R, Kumar R, (2011) Adsorption of Amaranth Dye onto Alumina Reinforced Polystyrene. *Clean-Soil, Air, Water* **39**, 74–82. https://doi.org/10.1002/clen.201000125

Aljeboree AM, Alshirifi AN, Alkaim AF, (2017) Kinetics and equilibrium study for the adsorption of textile dyes on coconut shell activated carbon. *Arab. J. Chem.* **10**, S3381–S3393. https://doi.org/10.1016/j.arabjc.2014.01.020

Annadurai G, Juang RS, Lee DJ, (2002) Use of cellulose-based wastes for adsorption of dyes from aqueous solutions. J Hazard Mater 92:263–274. https://doi.org/10.1016/S0304-3894(02)00017-1

Bai H, Zhang Q, He T, Zheng G, Zhang G, Zheng L, Ma S, (2016) Adsorption dynamics, diffusion and isotherm models of poly(NIPAm/LMSH) nanocomposite hydrogels for the removal of anionic dye Amaranth from an aqueous solution. *Appl. Clay Sci.* **124–125**,157–166. https://doi.org/10.1016/j.clay.2016.02.007

Chen H, Deng X, Ding G, Qiao Y, (2019) The synthesis, adsorption mechanism and application of polyethyleneimine functionalized magnetic nanoparticles for the analysis of synthetic colorants in candies and beverages. *Food Chem*. **293**, 340–347. https://doi.org/10.1016/j.foodchem.2019.04.111

Chiou MS, Li HY, (2002) Equilibrium and kinetic modeling of adsorption of reactive dye on cross-linked chitosan beads. *J. Hazard. Mater.* **93**, 233–248. https://doi.org/10.1016/S0304-3894(02)00030-4

El-Naggar ME, Radwan EK, El-Wakeel ST, Kafafy H., Gad-Allah TA, El-Kalliny AS, Shaheen TI. (2018) Synthesis, characterization and adsorption properties of microcrystalline cellulose based nanogel for dyes and heavy metals removal. I*nt. J. Biol. Macromol.* **113**, 248–258. https://doi.org/10.1016/j.ijbiomac.2018.02.126

Ge F, Ye H, Li MM, Zhao BX (2012) Efficient removal of cationic dyes from aqueous solution by polymer-modified magnetic nanoparticles. *Chem. Eng. J.* **198–199,** 11–17. https://doi.org/10.1016/j.cej.2012.05.074

Ghaedi M, Sadeghian B, Pebdani AA, Sahraei, R., Daneshfar, A., Duran, C. (2012) Kinetics, thermodynamics and equilibrium evaluation of direct yellow 12 removal by adsorption onto silver nanoparticles loaded activated carbon. *Chem. Eng. J.* **187**, 133–141. https://doi.org/10.1016/j.cej.2012.01.111

Godiya CB, Cheng X, Li D, Chen Z, Lu X, (2019) Carboxymethyl cellulose/polyacrylamide composite hydrogel for cascaded treatment/reuse of heavy metal ions in wastewater. *J. Hazard. Mater.* **364**, 28–38. https://doi.org/10.1016/j.jhazmat.2018.09.076

Guerrero-Coronilla I, Morales-Barrera L, Villegas-Garrido TL, Urbina EC, (2014) Biosorption of amaranth dye from aqueous solution by roots, leaves, stems and the whole plant of E. crassipes. *Environ. Eng. Manag. J.* **13**, 1917–1926. https://doi.org/10.30638/eemj.2014.212

Habeeb OA, Kanthasamy R, Ali GAM, Ali M., Yunus RM , Olalere OA, (2017) Kinetic, isotherm and equilibrium study of adsorption of hydrogen sulfide from wastewater using modified eggshells. *IIUM Eng. J.* **18**, 13–25. https://doi.org/10.31436/iiumej.v18i1.689

Ho YS, McKay G (1998) Sorption of dye from aqueous solution by peat. *Chem. Eng. J.* **70**, 115–124. https://doi.org/10.1016/S1385-8947(98)00076-X

Huang X, Luo X, Liu L, Dong K, Yang R, Lin C, Song H, Li S, Huang Q, (2020) Formation mechanism of egg white protein/κ-Carrageenan composite film and its application to oil packaging. *Food Hydrocoll.* **105**, 105780. https://doi.org/10.1016/j.foodhyd.2020.105780

Hussien MA, El-Bindary AA, El-Sonbati AZ, Shoair A, El-Boz RA (2016) Green removal of phenolic azo dye from aqueous solutions using rice straw fly ash. *J. Mater. Environ. Sci.* **7**, 4214–4225

Jiang H, Chen P, Zhang W, Luo S, Luo X, Au C, Li M, (2014) Deposition of nano Fe_3O_4@mZrO_2 onto exfoliated graphite oxide sheets and its application for removal of amaranth. *Appl. Surf. Sci.* **317**,1080–1089. https://doi.org/10.1016/j.apsusc.2014.09.023

Li N, Dang H, Chang Z, Zhao X, Zhang M, Li W, Zhou H, Sun C, (2019) Synthesis of uniformly

distributed magnesium oxide micro-/nanostructured materials with deep eutectic solvent for dye adsorption. *J. Alloys Compd.* **808**, 151571. https://doi.org/10.1016/j.jallcom.2019.07.283

Liao H, Wang Z (2018) Adsorption removal of amaranth by nanoparticles-composed Cu_2O microspheres. *J. Alloys Compd.* **769**, 1088–1095. https://doi.org/10.1016/j.jallcom.2018.08.088

Lin K-YA, Wu C-H, (2017) Efficient Adsorptive Removal of Toxic Amaranth Dye from Water using a Zeolitic Imidazolate Framework. *Water Environ. Res.* **90**, 1947–1955. https://doi.org/10.2175/106143017x14902968254692

Liu X, Zhang Q, Peng B, Ren Y, Cheng B, Ding C, Su X, He J, Lin S, (2020a) Flame retardant cellulosic fabrics via layer-by-layer self-assembly double coating with egg white protein and phytic acid. *J. Clean Prod.* **243,** 118641 https://doi.org/10.1016/j.jclepro.2019.118641

Liu X, Zhou Z, Yin J, He C, Zhao W, Zhao C (2020b) Fast and environmental-friendly approach towards uniform hydrogel particles with ultrahigh and selective removal of anionic dyes. *J. Environ. Chem. Eng.* **8**, 104352. https://doi.org/10.1016/j.jece.2020.104352

Long BT, (2020) Inverse algorithm for Streeter–Phelps equation in water pollution control problem. *Math Comput. Simul.* **171**, 119–126. https://doi.org/10.1016/j.matcom.2019.12.005

Long C, Jiang Z, Shangguan J, Qing T, Zhang P, Feng B, (2021) Applications of carbon dots in environmental pollution control: A review. *Chem. Eng. J.* **406**, 126848. https://doi.org/10.1016/j.cej.2020.126848

Lyu H, Hu K, Fan J, Ling Y, Xie Z, Li J, (2020) 3D hierarchical layered double hydroxide/carbon spheres composite with hollow structure for high adsorption of dye. *Appl. Surf. Sci.* **500**, 144037. https://doi.org/10.1016/j.apsusc.2019.14403

Mishra SP, Patra AR, Das S, (2021) Methylene blue and malachite green removal from aqueous solution using waste activated carbon. *Biointerface Res. Appl. Chem.* **11**, 7410–7421. https://doi.org/10.33263/BRIAC111.74107421

Mittal A, Mittal J, Malviya A, Kaur D, Gupta VK, (2010) Adsorption of hazardous dye crystal violet from wastewater by waste materials. *J. Colloid Interface Sci.* **343**, 463–473. https://doi.org/10.1016/j.jcis.2009.11.060

Ndifor-Angwafor NG, Kuete Tiotsop IH, Tchuifon Tchuifon DR, Sadeu CN, Bopda A, Anagho SG, Kamdem TA, (2017) Biosorption of amaranth red in aqueous solution onto treated and untreated lignocellulosic materials (pineapple peelings and coconut shells). *J. Mater. Environ. Sci.* **8**, 4199–4212. https://doi.org/10.26872/jmes.2017.8.12.441

Pandian P, Arivoli S, Marimuthu V, Prabaharan T, (2013) Adsorption of Cu (II) Ions from Aqueous Solution by Activated Ipomoea Carnea : Equilibrium Isotherms and Kinetic Approach. *Int. J. Eng. Innov. Technol.* **3**, 156–162

Qiao J, Gao S, Yao J, Zhang L, Li N, (2019) A rapid and green method for the removal of anionic dyes from aqueous solution using sulfobetaine-modified magnetic nanoparticles. *AIP Adv*. **9**, 065308 https://doi.org/10.1063/1.5101013

Salem ANM, Ahmed MA, El-Shahat MF, (2016) Selective adsorption of amaranth dye on Fe3O4/MgO nanoparticles. *J. Mol. Liq.* **219**, 780–788. https://doi.org/10.1016/j.molliq.2016.03.084

Shi H, Dong C, Yang Y, Han Y, Wang F, Wang C, Men J, (2020) Preparation of sulfonate chitosan microspheres and study on its adsorption properties for methylene blue. *Int. J. Biol. Macromol.* **163**, 2334–2345. https://doi.org/10.1016/j.ijbiomac.2020.09.078

Siyal AA, Shamsuddin MR, Low A, Rabat NE, (2020) A review on recent developments in the adsorption of surfactants from wastewater. *J. Environ. Manage.* **254**, 109797. https://doi.org/10.1016/j.jenvman.2019.109797

Sohni S, Hashim R, Nidaullah H, Lamaming Ja, Sulaiman O, (2019) Chitosan/nano-lignin based composite as a new sorbent for enhanced removal of dye pollution from aqueous solutions. *Int. J. Biol. Macromol.* **132**, 1304–1317. https://doi.org/10.1016/j.ijbiomac.2019.03.151

Soliman NK, Moustafa AF, (2020) Industrial solid waste for heavy metals adsorption features and challenges; a review. *J. Mater. Res. Technol.* **9**, 10235–10253. https://doi.org/10.1016/j.jmrt.2020.07.045

Sun D, Zhang X, Wu Y, Liu X, (2010) Adsorption of anionic dyes from aqueous solution on fly ash. *J. Hazard. Mater.* **181**, 335–342. https://doi.org/10.1016/j.jhazmat.2010.05.015

Wahba MI (2020) Mechanically stable egg white protein based immobilization carrier for β-D-galactosidase: Thermodynamics and application in whey lactose hydrolysis. *React. Funct. Polym.*

155, 104696. https://doi.org/10.1016/j.reactfunctpolym.2020.104696

Wang H, Li Z, Yahyaoui S, Hanafy H, Seliem MK, Bonilla-Petriciolet A, Dotto GL, Sellaoui, Li Q, (2020) Effective adsorption of dyes on an activated carbon prepared from carboxymethyl cellulose: Experiments, characterization and advanced modelling. *Chem. Eng. J.* 128116. https://doi.org/10.1016/j.cej.2020.128116

Weber TW, Chakravorti RK (1974) Pore and solid diffusion models for fixed-bed adsorbers. *AIChE J.* **20**, 228–238. https://doi.org/10.1002/aic.690200204

Wong S, Yac'cob NAN, Ngadi N, Ngadi N, Hassan O, Inuwa İB, (2018) From pollutant to solution of wastewater pollution: Synthesis of activated carbon from textile sludge for dye adsorption. *Chinese J. Chem. Eng.* **26**, 870–878. https://doi.org/10.1016/j.cjche.2017.07.015

Xu J, Du P, Bi W, Yao G, Li S, Liu H (2020) Graphene oxide aerogels co-functionalized with polydopamine and polyethylenimine for the adsorption of anionic dyes and organic solvents. *Chem. Eng. Res. Des.* **154**,192–202. https://doi.org/10.1016/j.cherd.2019.12.014

Zafar MN, Dar Q, Nawaz F, Zafar MN, Iqbal M, Zafar MF, (2019) Effective adsorptive removal of azo dyes over spherical ZnO nanoparticles. *J. Mater. Res. Technol.* **8**, 713–725. https://doi.org/10.1016/j.jmrt.2018.06.002

Zhou Z, Lin S, Yue T, Lee TC, (2014) Adsorption of food dyes from aqueous solution by glutaraldehyde cross-linked magnetic chitosan nanoparticles. *J. Food Eng.* **126**, 133–141. https://doi.org/10.1016/j.jfoodeng.2013.11.014